THE JOURNAL OF PHYSICAL CHEMISTRY A

Article

pubs.acs.org/JPCA

Substituent-Modulated Affinities of Halobenzene Derivatives to the HIV-1 Integrase Recognition Site. Analyses of the Interaction Energies by Parallel Quantum Chemical and Polarizable Molecular Mechanics

Krystel El Hage,[†,‡] Jean-Philip Piquemal,[§] Zeina Hobaika,[‡] Richard G. Maroun,[‡] and Nohad Gresh*[,†,§]

[†]Chemistry and Biology, Nucleo(s)tides and Immunology for Therapy (CBNIT), UMR 8601 CNRS, UFR Biomédicale, Paris 75006, France

[‡]Centre d'Analyses et de Recherche, UR EGFEM, LSIM, Faculté des Sciences, Saint Joseph University of Beirut, B.P. 11-514 Riad El Solh, Beirut 1107 2050, Lebanon

[§]Laboratoire de Chimie Théorique, UMR 7616 CNRS, UPMC, Sorbonne Universités, Paris 75005, France

ABSTRACT: The C−X bond of halobenzenes (X = Cl, Br) has a dual character, its electron density being depleted in its prolongation and built-up on its sides. We have recently considered three protein or nucleic acid recognition sites of halobenzenes and quantified the energy gains that either electron-attracting substituents or electron-donating ones contribute due to such a character (El Hage et al., paper in revision). Nonadditivity was found to impact the total interaction energies. We focus here on one recognition site, that of the HIV-1 integrase, in which the halobenzene ring of the drug elvitegravir is sandwiched between a guanine and a cytosine base. We perform energy-decomposition analyses of the ab initio quantum-chemistry (QC) binding energies of the parent halobenzene ring and its derivatives with this G−C base pair. In these complexes, the nonadditivity of ΔE could be traced back mostly to the polarization contribution E_{pol}. In view of large-scale applications to the entirety of the complex formed between the integrase, the viral DNA, and the whole drug, the analyses were performed in parallel with a polarizable molecular mechanics method, SIBFA. This method could faithfully reproduce most features of the QC energies. This is due to its use of QC-derived distributed multipoles and polarizabilities, which enable us to account for both nonisotropy and nonadditivity.

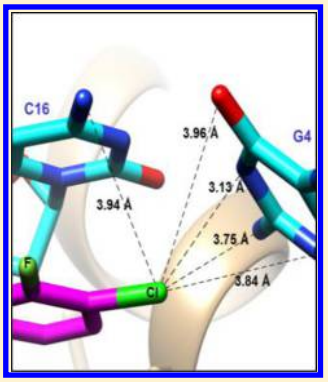

INTRODUCTION

Halogenated benzyl rings constitute an important moiety of several drugs and drug candidates in clinical use and development.[1−3] The presence of a "σ-hole", namely electron deficiency prolonging the CX bond (X = Cl, Br, I),[4−6] enables halobenzenes to target electron-rich sites of proteins and DNA receptors along such a bond. The concomitant buildup of electron density around the CX bonds could enable halobenzenes to target electron-deficient sites of such receptors as well, and several protein and DNA recognition sites of halobenzenes show the halobenzene residing in the neighborhood of electron-rich as well as electron-deficient sites of the receptor.[7−10]

We have recently considered three targets, namely farnesyl transferase, coagulation factor Xa, and HIV-1 integrase. Halobenzene binding to both kinds of sites could be enhanced by well-defined substituents that respectively deplenish or replenish the CX electron density [El Hage et al., paper in revision]. Comparisons with the parent compounds showed in addition some unanticipated features. One of these bore on the impact of polysubstitutions on the solvation energy ΔG_{solv}. Such polysubstitutions, in addition to increasing local electrostatic interactions with a targeted site, could in some cases reduce ΔG_{solv}, thus impacting favorably the energy balances. This was due to a reduction of the total molecular dipole moment, as occurs with, e.g., two identical substituents *para* with respect to one another. Instructive departures from nonadditivity were found in several cases as a consequence of polysubstitution. That is, the resulting energy gains with respect to the parent compound could be larger than the sum of the gains resulting from all monosubstitutions considered alone. Finally, the intermolecular interaction energies between the halobenzene derivatives and the two closest residues or DNA bases of the recognition site differed in magnitude from the sum of the three pairwise interactions, being either cooperative or anticooperative. Such a nonadditivity is a recurrent feature of multiply H-bonded complexes on the one hand, and of polycoordinated complexes of metal cations on the other hand, and has been previously analyzed by parallel quantum-chemistry (QC) and polarizable molecular mechanics (PMM) analyses (see ref 11 and references therein). To our knowledge, its occurrence in stacked complexes in protein or DNA recognition sites does not appear to have precedents.

Received: August 7, 2014
Revised: September 15, 2014
Published: September 17, 2014

Downloaded via UNIV PIERRE ET MARIE CURIE on May 12, 2019 at 14:01:09 (UTC).
See https://pubs.acs.org/sharingguidelines for options on how to legitimately share published articles.

 © 2014 American Chemical Society dx.doi.org/10.1021/jp5079899 | J. Phys. Chem. A 2014, 118, 9772−9782

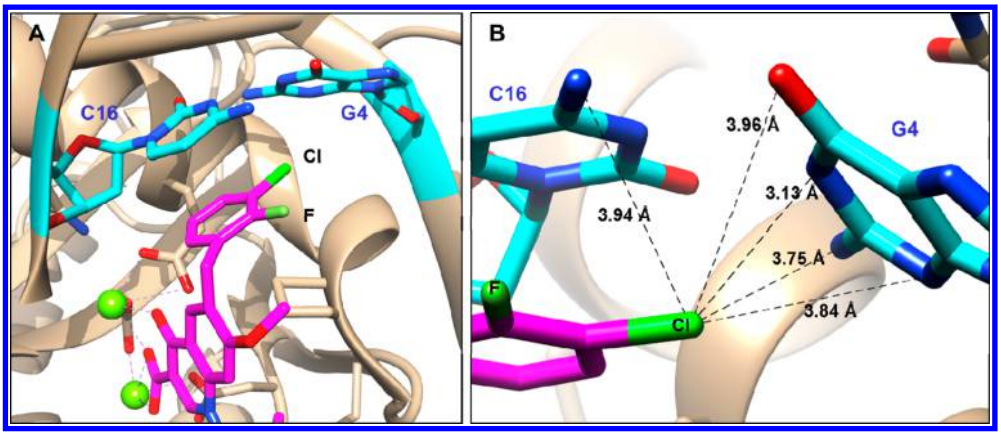

Figure 1. Representation of the INT−DNA-elvitegravir complex. (a) Recognition site of the halobenzene ring focusing on its interaction with G4 and C16 bases. (b) Interaction distances between the chlorine atom of elvitegravir and the two bases.

The present study focuses on the halobenzene recognition site of HIV-1 integrase, INT (1). INT is the enzyme responsible for the integration of viral DNA into host DNA and is the target of several efficient anti-HIV-1 drugs.[12] Among these, elvitegravir was developed by Gilead Sciences and has an in vitro EC_{90} of 1.7 nM.[13−15] It was FDA approved in 2012 for AIDS therapy.[16] The X-ray structure of its INT complex shows its chlorofluorobenzene ring stacked over a cytosine, while its CCl bond points toward the center of an electron-rich ring of a guanine.[17] The complex is represented in Figure 1a,b, the molecular structure of the drug being shown in Figure 1B. The present analysis can thus be limited to the halobenzene ring and its derivatives and to the C and G bases. We will quantify the weights of the individual contributions of the interaction energy by QC energy decomposition analyses at the HF level. The impact of correlation/dispersion is quantified upon passing to the correlated B97-D level. Simulations on the complexes of elvitegravir and its novel derivatives with the entirety of INT and bound DNA could only be done in the context of molecular mechanics/dynamics. The nonadditivity shown with the ternary complex, let alone the presence of two Mg(II) dications and of several structural waters in the entirety of the complex, render it necessary to resort to polarizable molecular mechanics. Specifically, we will run parallel analyses with the SIBFA anisotropic polarizable molecular mechanics (APMM) [reviewed in ref 11]. For the present purposes, there are two essential assets of this procedure: (1) Distributed multipoles are used to compute the electrostatic contribution and the polarizing field. This was shown to be instrumental to enable one to closely account for the pronounced in-plane and out-of-plane anisotropies of the QC Coulomb contribution.[11] (2) Distributed polarizabilities are used to compute the polarization contribution. Both distributed multipoles and polarizabilities are derived from the ab initio QC molecular orbitals of the individual molecules and molecular fragments. How closely could then an APMM method account for both nonisotropy and nonadditivity features of the QC intermolecular interaction energies, and to what an extent could each QC contributions be matched by its APMM counterpart?

METHODS

1. QC Computations. *Energy Decomposition Analysis.* The decomposition of the ab initio SCF interaction energy is done using the reduced variational space (RVS) analysis of Stevens and Fink.[18] This procedure separates the total interaction energy into four contributions (2): the first-order (E1) Coulomb (ES) and short-range exchange−repulsion (EX) and the second-order (E2) polarization (POL) and charge transfer (CT). The basis set superposition error (BSSE)[19,20] is evaluated within the virtual orbital space.

We used the GAMESS software[21] and the cc-pVTZ(-f) basis set.[22,23] This basis set was shown to reproduce closely the results from the more extended aug-cc-pVTZ basis set in several test calculations bearing on inter- as well as intramolecular interactions.[24]

Correlated Calculations. The intermolecular interaction energies ΔE were computed at the correlated level using the dispersion-corrected B97-D functional by Grimme and coworkers[25] with the G09 software[26] and the cc-pVTZ(-f) basis set. The values of ΔE were also corrected for BSSE. The use of the aug-cc-pVTZ basis set was hampered by convergence issues for several complexes and could not be pursued for the present work.

At both HF and DFT-d levels, nonadditivity was computed as the difference between the interaction energy of the ternary complex and the sum of the three pairwise interaction energies. For a given complex, the dispersion contribution (E_{disp}) is evaluated as the difference between the BSSE-corrected B97-D intermolecular interaction energies and the HF ones. The structures of all complexes, as well as those of the ligands taken in isolation, were energy-minimized using G09 using as a starting structure for the one determined by X-ray crystallography.

2. SIBFA Computations. In the SIBFA procedure,[11] the intermolecular interaction energy is computed as the sum of five contributions: electrostatic multipolar (E_{MTP}), short-range repulsion (E_{rep}), polarization (E_{pol}), charge transfer (E_{CT}), and dispersion (E_{disp})

$$\Delta E_{tot} = E_{MTP} + E_{rep} + E_{pol} + E_{CT} + E_{disp}$$

E_{MTP} is computed with distributed multipoles (up to quadrupoles) derived from the QC molecular orbitals precomputed for each individual molecule. They are derived from the Stone analysis[27,28] and distributed on the atoms and the bond barycenters using a procedure developed by Vigné-Maeder and Claverie.[29] This was done by a home-built routine (Devereux, M., Paris, 2010). It is augmented with a penetration term.[30] The anisotropic polarizabilities are distributed on the centroids of the localized orbitals (heteroatom lone pairs and bond barycenters) using a procedure due to Garmer and

dx.doi.org/10.1021/jp5079899 | J. Phys. Chem. A 2014, 118, 9772−9782

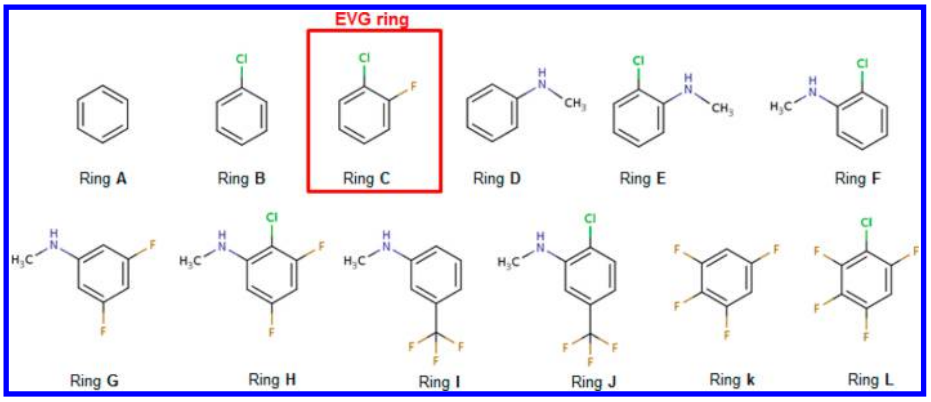

Figure 2. Representations of the investigated halobenzene derivatives.

Table 1. Nonadditivity Values of ΔE (kcal/mol) of Rings A, B, D, E, G, H, I, J, K, and L at the DFT Level with the B97-D Functional

ΔE_{gas} (kcal/mol)	ring A	ring B	ring D	ring E	ring G	ring H	ring I	ring J	ring K	ring L
$\sum$ binary complexes	−36.3	−39.2	−41.2	−42.2	−41.5	−47.4	−42.6	−48.6	−40.8	−41.7
ternary complex	−36.0	−38.9	−43.0	−43.4	−41.1	−44.0	−42.1	−45.2	−39.9	−40.6
nonadditivity	0.3	0.3	−1.8	−1.3	0.5	3.3	0.5	3.4	0.9	1.1

Table 2. Nonadditivities of the Individual HF Contributions Rings A, B, C, D, E, F, G, H, and L, Obtained from RVS Energy Decompositions

nonadditivity (kcal/mol)	ring A	ring B	ring C	ring D	ring E	ring F	ring G	ring H	ring L
ΔE_{tot}	0.1	−0.2	0.2	−1.8	−1.3	0.4	0.3	0.8	0.8
ES	0.0	0.0	0.0	0.0	0.0	0.0	0.0	0.0	0.0
EX	−0.3	−0.2	−0.2	−0.2	−0.1	−0.2	0.0	0.2	−0.1
E_{pol}(RVS)	0.3	0.2	0.5	−0.8	−0.5	0.5	0.3	0.6	0.7
E_{pol}(KM)	0.3	0.1	0.4	−1.7	−1.2	0.4	0.1	0.4	0.7
CT	0.1	0.1	0.2	0.0	0.1	0.2	0.1	0.2	0.2
E1	−0.3	−0.2	−0.2	−0.2	−0.1	−0.2	0.0	0.2	−0.1
E2	0.4	0.2	0.7	−1.6	−1.1	0.5	0.2	0.5	0.9

Stevens.[31] The parameters for F and Cl have been previously calibrated so that ΔE(SIBFA) matches ΔE(RVS) upon Mg^{2+} and water approach along the CX bond and the corresponding equilibrium distances match to within 0.1 Å.[32] E_{rep} and E_{CT}, the two short-range repulsions, are computed using representations of the molecular orbitals localized on the chemical bonds and on localized lone-pairs. E_{disp} is computed as an expansion into $1/R^6$, $1/R^8$, and $1/R^{10}$, and also embodies an explicit exchange−dispersion term.[33]

RESULTS AND DISCUSSION

Energy Calculations. Along with ring A, namely unsubstituted benzene, Figure 2 recasts the 11 halobenzenes whose binding affinities were compared in a preceding study [El Hage et al., paper in revision]. One *meta* position to chlorine is left unsubstituted, because in complete elvitegravir, it is used for the connection to the rest of the molecule. Ring C, with a fluorine *ortho* to the chlorine, is the representative of elvitegravir. This group of compounds encompasses rings with one electron-donating group, *N*-methylamine, on either side of the Cl atom, as in rings E and F. It can also encompass electron-withdrawing groups, namely two or four fluorines or a trifluoromethyl group. These can coexist with the *N*-methylamine substituent, as in rings G, L, and I, or substitute without it, as in rings K and L. For each kind of substitution, the nonchlorinated analog is considered as well, to evaluate the mutual impacts of chlorination and substitution on the binding affinities.

We present first an analysis of the nonadditivity of ΔE, by comparing its values in the ternary complexes with the G and C bases simultaneously to the ΔE sums of the three binary complexes. Table 1 recasts first the values found at the correlated level with the B97-D functional.

For nine selected derivatives, Table 2 lists the nonadditivities of the individual HF contributions obtained from the energy decompositions. Two values are given for E_{pol}. These are E_{pol}(RVS), resulting from SCF iterations in which each monomer is relaxed while the others are frozen, and E_{pol}(KM) as computed by the Kitaura−Morokuma (KM) procedure,[34] in which all monomers are relaxed simultaneously.

It is first observed that the three rings enabling the largest energy gains with respect to the parent compound are E, H, and J. Ring E has solely an electron donor, −NHCH3, *ortho* to chlorine, whereas rings H and J have the −NHCH3 group coexisting with electron attractors, namely two F atoms *ortho* and *para* to Cl in ring H and a trifluoromethyl group *para* to it in ring J. These compounds enable energy gains in the range −5.1 to −6.9 kcal/mol with respect to the parent compound. For ring E, chlorination results in a weak (−0.4 kcal/mol) energy gain with respect to unchlorinated ring D. By contrast, chlorination enables −3 kcal/mol energy gains, both for ring H as compared to unchlorinated ring G and for ring J as compared to I. This could be a reflection of the "Janus-like"

dx.doi.org/10.1021/jp5079899 | J. Phys. Chem. A 2014, 118, 9772−9782

Table 3. SIBFA versus QC Energy Decomposition Calculations (kcal/mol) (a) for the Ternary and the Binary Complexes of Rings A, C, D, E, G, H, and L and (b) for the Complexes with the Sole Cytosine or Guanine Rings

	ring A		ring C		ring D		ring E		ring G		ring H		ring L	
E (kcal/mol)	SIBFA	QC	SIBFA	QC	SIBFA	QC	SIBFA	QC	SIBFA	QC	SIBFA	QC	SIBFA	QC
						C−G Ring								
E_{MTP}	−33.9	−33.0	−32.7	−32.6	−37.3	−37.9	−37.5	−37.7	−36.6	−36.4	−36.4	−35.7	−35.7	−33.5
E_{rep}	27.1	27.4	25.0	26.4	26.4	27.1	26.9	27.3	29.3	29.0	30.2	30.9	28.0	27.8
E1	−6.8	−5.6	−7.7	−6.2	−11.0	−10.8	−10.6	−10.3	−7.3	−7.4	−6.1	−4.7	−7.7	−5.7
E_{pol}*/E_{pol}(RVS)	−5.9	−6.0	−5.6	−6.0	−8.3	−8.5	−8.4	−8.1	−6.2	−6.5	−6.3	−6.4	−5.7	−5.7
E_{pol}/E_{pol}(KM)	−6.8	−7.5	−6.5	−7.4	−10.0	−11.0	−10.2	−10.5	−7.3	−8.2	−7.3	−8.1	−6.6	−7.3
E_{CT}*	−2.0	−3.0	−1.9	−2.9	−3.3	−3.5	−3.4	−3.6	−2.5	−3.5	−2.3	−3.5	−5.6	−3.1
E_{CT}		−4.2		−4.2		−4.6		−4.7		−4.8		−5.0		−4.9
Δ*E*	**−15.6**	**−17.1**	**−16.1**	**−17.9**	**−23.6**	**−26.3**	**−23.2**	**−25.4**	**−17.1**	**−20.2**	**−15.9**	**−17.6**	**−17.5**	**−17.5**
E_{disp}	−21.0	−19.0	−21.0	−20.4	−18.3	−16.8	−18.6	−18.0	−23.3	−20.9	−26.6	−26.4	−23.1	−23.1
ΔE_{tot}[a]	**−36.6**	**−36.0**	**−37.1**	**−38.3**	**−41.8**	**−43.0**	**−41.9**	**−43.4**	**−40.4**	**−41.1**	**−42.6**	**−44.0**	**−40.8**	**−40.6**
ΔE_{tot}[b]		**−33.3**		**−34.0**		**−41.9**		**−41.1**		**−38.2**		**−40.3**		**−36.2**
ΔE_{tot}[c]		**−33.9**		**−34.9**		**−42.0**		**−41.5**		**−39.7**		**−42.9**		**−38.2**
						C Ring								
E_{MTP}	−1.1	−0.4	−3.03	−3.24	−4.2	−4.8	−2.9	−3.4	−9.4	−8.2	−8.6	−7.0	−3.0	−1.3
E_{rep}	5.3	5.6	6.05	6.53	5.4	5.8	6.0	6.3	11.5	11.6	11.2	10.7	4.8	4.2
E1	4.2	5.2	3.0	3.3	1.3	1.0	3.1	2.9	2.1	3.4	2.6	3.6	1.8	2.9
E_{pol}*/E_{pol}(RVS)	−0.4	−0.5	−0.54	−0.6	−0.7	−0.9	−0.7	−0.9	−0.9	−1.1	−0.8	−1.1	−0.5	−0.6
E_{pol}/E_{pol}(KM)	−0.4	−0.6	−0.54	−0.7	−0.7	−1.3	−0.8	−1.2	−1.0	−1.3	−0.9	−1.3	−0.5	−0.7
E_{CT}*	0.0	−0.1	0.00	−0.21	−1.1	−0.6	−1.1	−0.5	−0.1	−0.7	−0.1	−0.8	−0.1	−0.1
E_{CT}		−0.5		−0.79		−0.8		−0.8		−1.4		−1.5		−0.6
Δ*E*	**3.7**	**4.2**	**2.48**	**1.87**	**−0.5**	**−0.9**	**1.2**	**1.1**	**1.1**	**0.8**	**1.7**	**0.9**	**1.1**	**1.8**
E_{disp}	−7.0	−7.9	−9.9	−9.3	−4.9	−5.4	−5.3	−6.9	−11.9	−12.3	−13.7	−15.6	−6.4	−6.8
ΔE_{tot}[a]	**−3.3**	**−3.7**	**−7.4**	**−7.4**	**−5.9**	**−6.7**	**−4.0**	**−5.8**	**−10.8**	**−11.5**	**−12.1**	**−14.7**	**−5.3**	**−5.0**
						G Ring								
E_{MTP}	−4.6	−3.3	−1.13	−0.08	−5.6	−3.7	−7.0	−5.1	1.3	1.0	0.8	1.5	−3.5	−3.0
E_{rep}	6.9	6.7	3.93	4.74	6.0	5.5	5.9	5.9	2.8	2.1	4.0	3.9	8.4	8.4
E1	2.3	3.4	2.8	4.7	0.4	1.7	−1.0	0.8	4.2	3.2	4.8	5.3	4.9	5.4
E_{pol}*/E_{pol}(RVS)	−0.6	−0.4	−0.29	−0.55	−1.9	−1.5	−2.3	−1.5	−0.6	−0.5	−0.8	−0.6	−0.8	−0.6
E_{pol}/E_{pol}(KM)	−0.7	−0.7	−0.30	−0.65	−2.0	−1.6	−1.7	−1.7	−0.6	−0.5	−0.8	−0.6	−0.8	−0.8
E_{CT}*	−0.1	−0.2	−0.01	−0.16	−0.4	−0.3	−0.5	−0.4	−0.5	−0.1	−0.5	−0.2	0.0	−0.4
E_{CT}		−0.6		−0.53		−0.7		−0.8		−0.4		−0.5		−1.3
Δ*E*	**1.9**	**2.3**	**2.50**	**3.6**	**−1.5**	**−0.6**	**−3.1**	**−1.7**	**3.1**	**2.3**	**3.6**	**4.3**	**3.5**	**3.5**
E_{disp}	−5.8	−7.6	−3.3	−8.0	−4.7	−6.6	−5.2	−7.4	−3.2	−5.0	−4.7	−9.6	−9.4	−12.9
ΔE_{tot}[a]	**−3.9**	**−5.3**	**−0.8**	**−4.4**	**−6.2**	**−7.2**	**−8.4**	**−9.0**	**−0.1**	**−2.7**	**−1.1**	**−5.4**	**−6.2**	**−9.3**

	C−G	
E (kcal/mol)	SIBFA	QC
E_{MTP}	−28.6	−29.2
E_{rep}	15.3	15.3
E1	−13.3	−13.9
E_{pol}*/E_{pol}(RVS)	−5.1	−5.3
E_{pol}/E_{pol}(KM)	−6.0	−6.5
E_{CT}*	−1.9	−2.7
E_{CT}		−3.2
Δ*E*	**−21.2**	**−23.6**
E_{disp}	−7.9	−3.8
ΔE_{tot}[a]	**−29.0**	**−27.3**

[a]B97-D functional. [b]WB97X functional. [c]M062X functional.

character of the C−Cl bond lending itself to energy gains due to simultaneous enrichment of the electron density on the sides of the CX bond and its depletion in its prolongation. Rings E, H, and J are also those which among the chlorinated compounds give rise to the largest nonadditivities, but these are contrasted. We denote by "cooperative" those ternary complexes for which the interaction energy has a larger magnitude (ΔE more attractive) than the sum of the interaction energies of the three binary complexes, and by "anticooperative" those in which it is less attractive than it. Thus, whereas the complex of ring E is cooperative (δE = −1.3 kcal/mol), those of rings H and J are anticooperative (δE = 3.3 kcal/mol). Chlorination appears to be systematically detrimental to cooperativity, which can be seen upon comparing the δE trends in the nonchlorinated versus chlorinated analogues (e.g., rings D versus E, G versus H, and I versus J). Analysis of cooperativity was pursued for representative rings A−H and L upon performing RVS energy decompositions at the Hartree−Fock level, which to our knowledge is presently the only approach available to analyze complexes of more than two

dx.doi.org/10.1021/jp5079899 | J. Phys. Chem. A 2014, 118, 9772−9782

interacting molecules. It is reported in Table 2. Table 2 shows that the nonadditivity of ΔE(RVS) originates predominantly from polarization. The values of E_{pol}(RVS) and E_{pol}(KM) are comparable, except for the cooperative complexes of rings D and E, for which E_{pol}(KM) contributes twice as much as E_{pol}(RVS) to cooperativity. The nonadditivity of E_{exch} never exceeds 0.3 kcal/mol in magnitude and is generally compensated by that of E_{CT}.

It is noted that the nonadditivities at the RVS/HF level reflect closely those found at the B97-D level, with the exception of ring H, where it is significantly larger at the B97-D level than at the RVS one, namely 3.3 kcal/mol as compared to 0.6 kcal/mol. Nevertheless, the magnitude of this effect could be to some extent dependent upon the nature of the functional. Thus, as observed by El Hage et al. (paper in revision), it was reduced to 2.4 and 1.8 kcal/mol upon resorting to the WB97-X[35] and M06-2X[36] functionals.

It will be essential to subsequently evaluate if the predicted gains in affinity could be retained upon passing to the entirety of the INT−DNA complex, and following inclusion of the ring derivatives in the entire elvitegravir group as a replacement for parent ring C. QC calculations are not tractable for such large complexes. MM approaches should be able to handle both the nonadditivity issue and the anisotropy of the energy surface around the CX bond due to the σ-hole. The first issue is only amenable to treatments by polarizable MM. The second should be most safely handled upon resorting to distributed multipole treatments.[32,37] For such reasons, we have resorted to the SIBFA procedure, which computes the electrostatic and polarization contributions with distributed QC multipoles and polarizabilities. The use of multipoles should enable us to account for the modulation of the electrostatic contribution as a function of the electron-donating or -withdrawing nature of the substituents, and how it evolves upon passing from mono- to polysubstitution. The use of QC polarizabilities, along with the fact that the polarizing field is itself computed with distributed multipoles, should enable us to account for the related modulations of E_{pol} and of its nonadditivity.

Table 3 regroups the SIBFA versus QC calculations for the complexes of rings A, D, E, G, H, and L. As with the QC computations, two values are given for E_{pol}. The first, denoted as E_{pol}*, corresponds to the polarization energy in which each monomer is polarized by the field due to the permanent multipoles on the others. To compute the second, denoted as E_{pol}, the polarizing field on each monomer is computed in an iterative fashion, upon including the contributions due to the induced dipoles on the other monomers from the preceding iteration. Thus, for consistency with the QC computations, E_{pol}* is to be compared to E_{pol}(RVS) and E_{pol} is to be compared to E_{pol}(KM). The results for the ternary complexes are listed first. They are followed by the corresponding results with the sole cytosine and guanine rings. We denote by $E_{corr/disp}$(QC) the increment of interaction energy observed upon passing from the HF level to the B97-D one. In the ternary complexes, the two first-order contributions, E_{MTP} and E_{rep}, are seen to reproduce closely their RVS counterparts, EC and E_{exch}. E_{pol}*, which denotes the polarization contribution prior to performing the iterations on the induced dipoles, itself reproduces closely E_{pol}(RVS). E_{pol}, which results from such iterations, increases in magnitude similarly to E_{pol}(KM), but its magnitude is smaller. This could be due to the fact that E_{pol}(KM) tends to overestimate the "true" polarization energy owing to the nonorthogonalization of the MO's of the monomers during the KM procedure. E_{CT} has magnitudes close to those of E_{CT}*, which denotes the value of the RVS contribution after the BSSE correction. Such term-to-term agreements enable ΔE(SIBFA) to closely reproduce ΔE(RVS). Comparable agreements are observed for the binary complexes of the rings with cytosine and guanine. In turn, E_{disp}(SIBFA) in the ternary complexes reproduces closely $E_{corr/disp}$(QC), with the exception of ring H, for which a difference of 3.4 kcal/mol is observed. A lesser agreement is seen, however, for the binary complexes. In these, E_{disp}(SIBFA) appears to underestimate $E_{corr/disp}$(QC) for the complexes of the rings with guanine and with cytosine but, conversely, overestimates in the guanine−-cytosine complex. This indicates the possibilities and limitations of the present formulation of E_{disp}(SIBFA), considering that in the present study it was not refit to handle aromatic−aromatic interactions or halogen interactions. Ongoing refinements include the use of correlated multipoles and polarizabilities and augmenting the exchange-dispersion term by contributions from the lone pairs (Gresh et al., work in progress). They will be reported in due course.

Could E_{pol}(SIBFA) reproduce the nonadditivity of E_{pol}(QC)? This evaluation is given in Table 4. It shows that the nonadditivities of both E_{pol}(KM) and E_{pol}(RVS) are closely reproduced by their SIBFA counterparts. This outcome is fully consistent with results previously published on cooperative[38−40] as well as anticooperative[41,42] complexes. It is recalled that E_{CT}(SIBFA) is also nonadditive, but consistent with QC, this appears essentially in charged complexes. Although E_{rep} is additive, nonadditivity could be conferred by the explicit introduction of three-atom exponentials, as was done in the complexes of metal cations.[43] The nonadditivities of both contributions are found by QC to be negligible in the present complexes and will thus not be investigated further. In a forthcoming work, we will investigate the impact on non-additivities of using correlated multipoles and polarizabilities.

Table 4. Compared Nonadditivities of Both E_{pol}(KM) and E_{pol}*(RVS) with Their SIBFA Counterparts

	ΔE		E_{pol}/E_{pol}(KM)		E_{pol}*/E_{pol}(RVS)	
nonadditivity (kcal/mol)	SIBFA	QC	SIBFA	KM	SIBFA	RVS
ring A	0.3	0.1	0.2	0.3	0.3	0.3
ring D	−1.1	−1.8	−1.2	−1.6	−0.7	−0.8
ring E	−0.9	−1.3	−1.0	−1.2	−0.4	−0.5
ring G	0.1	0.3	0.2	0.1	0.3	0.3
ring H	0.7	0.6	0.4	0.4	0.4	0.6
ring L	0.9	0.8	0.8	0.7	0.8	0.7

Figures 3 give graphical comparisons of the QC and SIBFA interaction energies for the complexes of the five rings in the six ternary and the 12 binary complexes. Figure 3a first compares the values of ΔE(RVS) and ΔE(SIBFA). Figure 3b compares the corresponding evolutions of E1 and E2. Panels c−h of Figure 3 compare the evolutions of the individual contributions: EC and E_{MTP}; E_{exch} and E_{rep}; E_{pol}(RVS) and E_{pol}*; E_{pol}(KM) and E_{pol}; E_{CT}(QM) and E_{CT}(SIBFA); $E_{corr/disp}$(QC) and E_{disp}(SIBFA). Finally, Figure 3i compares the evolutions of ΔE_{tot}(QC) and ΔE_{tot}(SIBFA).

The evolutions of ΔE(SIBFA) reproduce closely those of ΔE(RVS). This is also the case for E1 and E2, as shown in Figure 3b, where it is clear that both contributions are needed

dx.doi.org/10.1021/jp5079899 | J. Phys. Chem. A 2014, 118, 9772−9782

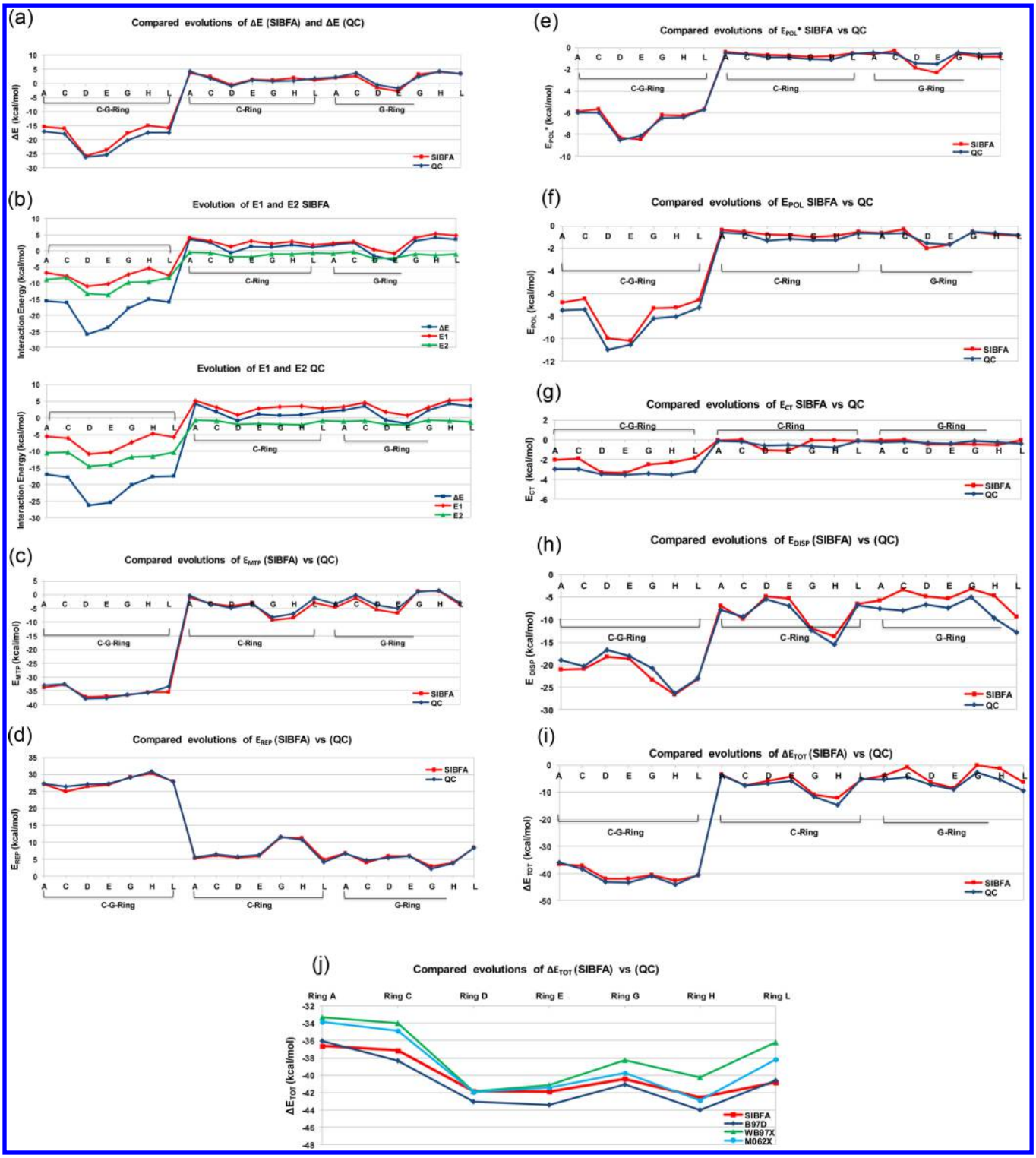

Figure 3. Compared evolutions of QC and SIBFA interaction energies and their individual contributions in the 18 investigated complexes: (a) ΔE(RVS) and ΔE(SIBFA); (b) E1 and E2; (c) EC and E_{MTP}; (d) E_{exch} and E_{rep}; (e) E_{pol}(RVS) and E_{pol}; (f) E_{pol}(KM) and E_{pol}; (g) E_{CT}; (h) $E_{corr/disp}$(QC) and E_{disp}(SIBFA); (i) ΔE_{tot}(QC/B97-D) and ΔE_{tot}(SIBFA); (j) ΔE_{tot}(QC) with the B97-D, WB97X, and M062X functionals and ΔE_{tot}(SIBFA).

to confer its shape to ΔE. *For all 18 complexes, whether ternary or binary, the stabilization due to the summed second-order term E2 is larger than that due to the first-order term E1.* This reemphasizes the need to explicitly include the polarization contribution. Within E1, both E_{MTP} and E_{rep} reproduce the trends of their QC counterparts, and the curves are virtually superimposable except for the binary complexes of D and E with guanine (Figure 3c,d). Although E_{pol}(SIBFA) can also closely reproduce the evolutions of E_{pol}(RVS), a slightly lesser agreement could be observed for the ternary complexes of D, G, and H, although the differences remains less than 1 kcal/mol. E_{CT}(SIBFA) is for some complexes underestimated by 1

dx.doi.org/10.1021/jp5079899 | J. Phys. Chem. A 2014, 118, 9772−9782

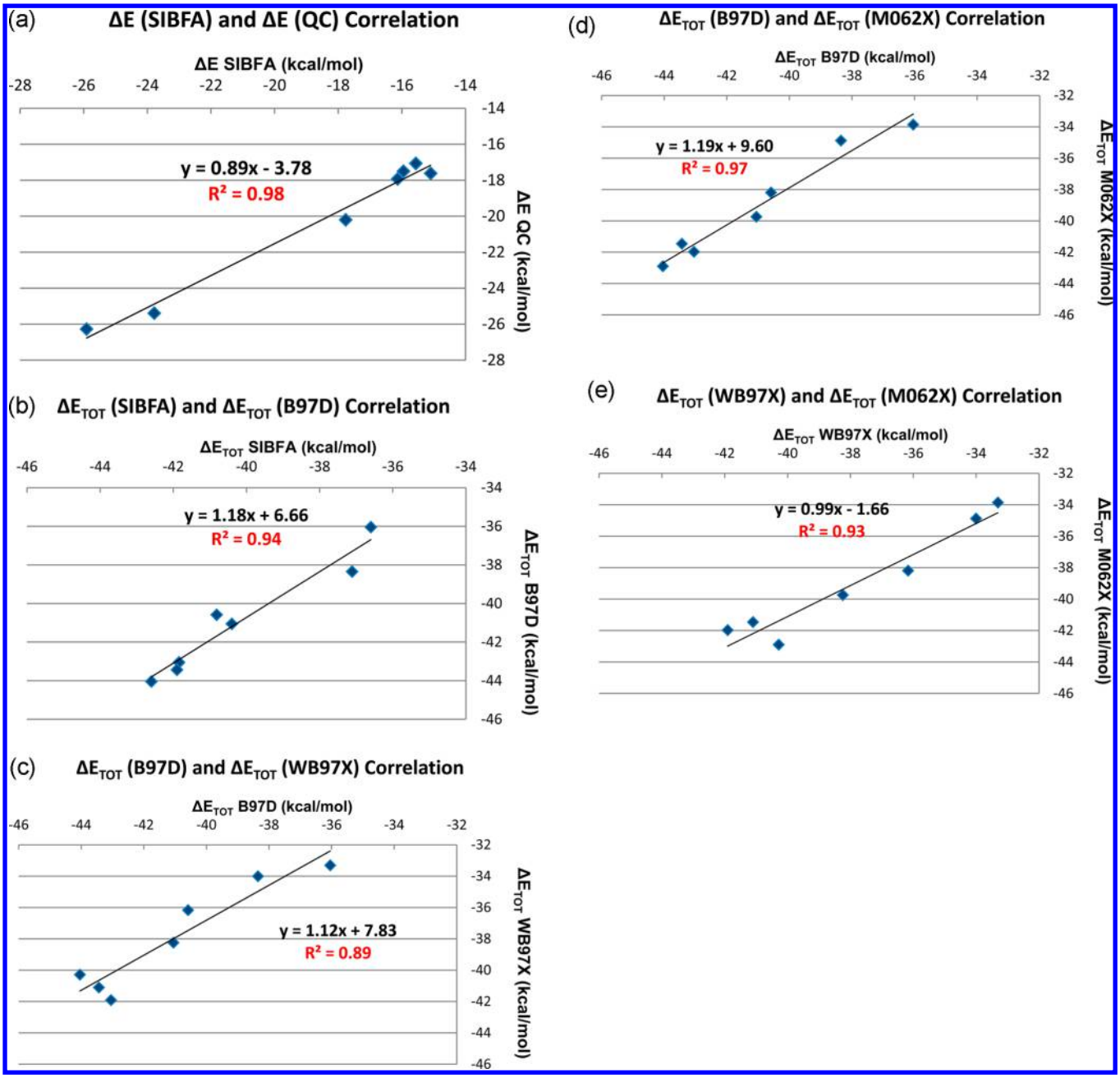

Figure 4. Correlations between the interaction energies of rings A, C, D, E, G, H, and L in the ternary complex as computed using SIBFA or three DFT functionals: (a) ΔE(SIBFA) and ΔE(QC/HF); (b) ΔE_{tot}(SIBFA) and ΔE(QC/B97-D); (c) ΔE(QC/B97-D) and ΔE(QC/WB97X); (d) ΔE(QC/B97-D) and ΔE(QC/M062X); (e) ΔE(WB97X) and ΔE(QC/M062X).

kcal/mol with respect to E_{CT}(RVS). This could illustrate some difficulties expressing the contributions of the π lone pairs to charge transfer (as is the case for ring A), and possibly also the need for a more focused calibration of E_{CT} contributed by the σ lone pairs of the fluorine substituents, as is the case for rings G, H, and L. In the ternary complexes, E_{disp}(SIBFA) can reproduce $E_{corr/disp}$(QC) closely, except for the case of ring H. The trends are also followed in the binary complexes. For these, as mentioned above, the underestimation of $E_{corr/disp}$(QC) by E_{disp}(SIBFA) is compensated by a corresponding overestimation in the G−C complex. As a consequence of the overall satisfactory agreements at the level of the individual contributions, ΔE_{tot}(SIBFA) can closely match ΔE_{tot}(QC), with the exception of ring H. On the other hand, the values of ΔE_{tot}(QC) can be sensitive to the choice of the functional. Thus, with the WB97-X functional, the ordering of ΔE_{tot}(QC) values is reversed, and their values are closer to the values of ΔE_{tot}(SIBFA).

For the seven rings considered, we have in Figure 4a plotted the evolutions of ΔE(SIBFA) against those of ΔE(RVS) in the form of a scatter plot. The close agreement is translated by a slope of 0.89 and an r^2 correlation of 0.98. The agreement is somewhat lesser upon comparing ΔE_{tot}(SIBFA) to ΔE(B97-D), with a slope of 1.18 and an r^2 of 0.94. This could translate the need for an improved formulation of E_{disp}(SIBFA) and/or the need to resort to distributed multipoles and polarizabilities, and work is in progress along both lines (Gresh et al., manuscript in preparation). We could nevertheless note that,

dx.doi.org/10.1021/jp5079899 | J. Phys. Chem. A 2014, 118, 9772−9782

with the exception of ΔE(B97-D) versus ΔE(M062X) giving a slope of 1.19 and r^2 of 0.97 (Figure 4d), the scatter between some functionals could be even larger than the present one, such as that between ΔE(B97-D) and ΔE(WB97X) with an r^2 of 0.89 (Figure 4c), or that between ΔE(WB97X) and ΔE(M062X),with an r^2 of 0.93 (Figure 4e). While this work was in progress, a paper appeared[44] benchmarking the accuracies of several DFT and dispersion-corrected DFT functionals for the interactions of small halogenated molecules with the benzene ring, as compared to CCSD(T)/CBS calculations. The M062X functional was found to afford better agreements for chlorinated compounds than B97-D. This should not alter the essential conclusions of this work aiming to compare the trends of ΔE as a function of chemical substitution as well as those of the separate first- and second-order contributions within ΔE. Furthermore, for the present class of compounds, ΔE(B97-D) could be seen to have a very satisfactory agreement with ΔE(M062X) with a 0.97 value of r^2.

Possible Impact of the Molecular Dipole Moment and of the Polarizability on Nonadditivity. The propensity of some of the substituted rings for nonadditivity in the G−C recognition site was unanticipated. Such effects could be amplified in the complete INT−DNA complex, because the two Mg(II) metal cations, as well as charged or polar residues neighboring the complexed DNA bases or the drug could further increase the magnitude of the polarizing field and, depending upon the field direction, amplify either cooperativity or anticooperativity. An ideal derivative would be one giving rise to cooperativity, which has only be obtained so far with derivatives D and E. Would it then be possible to anticipate the amplitude and nature of the nonadditive response from some molecular properties such as the molecular dipole or the molecular polarizability? Table 5 reports the value of δE_{nadd} as a function of the dipole moment of the ring and its polarizability for 19 substituted rings, nine of which are represented in Figure 2 (Table 5 top), and for ten additional substituted rings (Table 5 bottom). Figure 5 gives a map in which the amplitude of nonadditivity, δE_{nadd}, is given as a function of these two properties. Increasing the molecular polarizability increases the magnitude of δE_{nadd}. Thus, for a value of the dipole moment (μ) of 2.8 D, it increases in magnitude from 0.3 to 0.8 to 1.3 kcal/mol as the polarizability increases from 78 Å^3 to 96−105. The latter increase gives rise to a cooperativity instead of anticooperativity. On the other hand, increasing μ also increases nonadditivity but favors anticooperativity. Thus, for a polarizability of 90 Å^3, δE_{nadd} increases from 1.1 to 1.7 kcal/mol upon increasing μ by 3 D, from 4 to 7 D. For a polarizability of 96 Å^3, it increases from 0.8 to 3.6 and 3.7 kcal/mol upon increasing μ from 2.5 to 4.5 and 6 D. For a polarizability of 105 Å^3, it increases in magnitude (and becomes anticooperative) from 1.3 to 3.3 kcal/mol upon increasing μ from 2.5 to 5 D. The trends are clearly preliminary at this stage because they are in an environment limited to the two closest sites to the halogenated ring, namely guanine and cytosine. It could be very instructive to monitor how they evolve, on the one hand, in the more complex environment of the protein that has anionic residues and two metal cations at less than 8 Å from the ring and, on the other hand, in the presence of the field generated by the other molecular fragments that make up the drug (Figure 1). This could further highlight the need for polarizable potentials and is the object of ongoing work [El Hage, K., work in progress].

Table 5. Representation of the Nonadditivity δE_{nadd} in the Ternary Complexes as a Function of the Ring Molecular Dipole and Polarizability of the (Top) Majority of Rings Shown in Figure 2 and (Bottom) Several Other Substituted Rings

substituted rings	polarizability	μ (Debye)	ΔE_{nadd} (kcal/mol)
ring A	61.77	0.06	0.30
ring B	75.60	2.68	0.30
ring C	75.02	3.65	0.84
ring E	104.08	2.54	−1.27
ring F	95.94	2.63	0.82
ring G	83.37	4.90	0.47
ring H	102.88	4.84	3.32
ring J	116.49	3.97	3.39
ring L	80.51	1.85	1.08
substituted rings	polarizability	μ (Debye)	δE_{nadd} (kcal/mol)
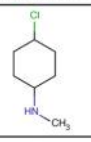	97.77	5.86	3.66
	78.27	1.05	0.91
	90.04	6.96	1.66
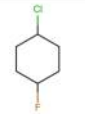	74.11	0.56	1.00
	78.91	4.52	0.83
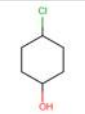	78.82	3.64	-0.30
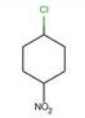	91.40	3.98	1.13
	97.22	4.54	3.55
	74.32	2.33	1.08
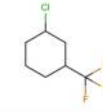	85.86	3.11	0.96

CONCLUSIONS AND PERSPECTIVES

The present study has focused on the halobenzene ring of elvitegravir, an inhibitor of HIV-1 integrase (INT), which has an in vitro EC_{90} of 1.7 nM and is presently used in therapy against AIDS. In the INT−DNA recognition site, this ring binds inside a cleft formed by a cytosine and a guanine. In line

dx.doi.org/10.1021/jp5079899 | J. Phys. Chem. A 2014, 118, 9772−9782

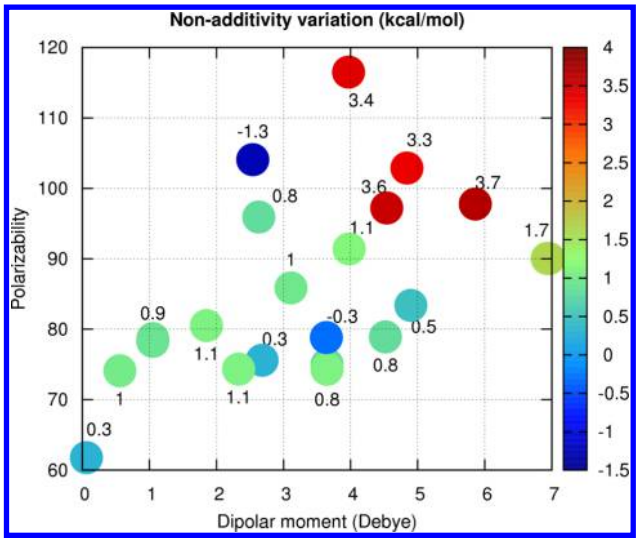

Figure 5. Representation of the magnitude of nonadditivity in the ternary complexes as a function of the ring molecular dipole and polarizabilty.

with a study by El Hage et al. (paper in revision), we considered halobenzene rings having different or additional substituents, some of which could give rise to significant energy gains (up to −5 kcal/mol) with respect to the parent chloro-*ortho* fluoro parent compound. QC energy-decomposition analyses were done to identify the energy contributions affording such gains. It was found at the HF level that the electrostatic contribution EC alone does not suffice to dictate the trends. On the one hand, its preferences could be either reinforced or counteracted within E1 by the short-range repulsion E_{exch}. On the other hand, the polarization contribution E_{pol} displayed preferential trends of its own, which could, again, either reinforce or counteract those of EC or E_{exch}. This appeared clearly upon comparing the evolution of ΔE(RVS) as a function of the considered ring derivative to those of the separate first- and second-order terms E1 and E2. None of the E1 and E2 curves alone could match the ΔE(RVS) curve and had to complement one another. In addition, E2 had invariably larger (or at least equal) magnitudes than E1. Furthermore, for some complexes, E_{pol} displayed some significant nonadditivities. Although these are a hallmark of several multiply H-bonded complexes and polycoordinated complexes of metal cations, their occurrence in stacked complexes is much rarer. They are most likely facilitated here by the fact that the two bases interacting with the ring are themselves mutually interacting by the Watson−Crick triple H-bond. Upon passing to the B97-D correlated level, $E_{corr/disp}$ displayed again some preferences of its own.

In view of large-scale simulations on the complexes that the entirety of the drug derivatives form with INT and its bound DNA, and due to the large size of the INT−DNA recognition site beyond the sole G4 and C16 bases, molecular mechanics/dynamics methods could be the most important surrogate to QC. The distinct preferences imposed by the separate energy contributions, the nonadditivities of ΔE, and the strongly anisotropic nature of the binding around the CX bond due to the σ-hole, imply that MM procedures equipped with a separable expression of ΔE, along with distributed QC multipoles and polarizabilities, as done by SIBFA and the effective fragment method[45,46] could be necessary. We have accordingly tested the SIBFA procedure and compared the numerical values and the evolutions of each of its five contributions to the QC ones, and close agreements could be seen in the majority of complexes. One possible exception relates to E_{disp} in the complex of ring H, which lacks the nonadditive behavior of its $E_{corr/disp}$ counterpart using the B97-D functional. However, the magnitude of such a nonadditivity was reduced with another functional, WB97X. It was, on the other hand, very encouraging to observe that the non-additivities of E_{pol}, whether from the RVS or from the KM approaches, could be reproduced by E_{pol}* and E_{pol}, respectively, that is, before and after iterating on the induced dipoles.

Following these validations, we have initiated simulations on the complexes of DNA-bound INT with elvitegravir derivatives with rings A−H, and the results will be reported subsequently.

AUTHOR INFORMATION

Corresponding Author

*N. Gresh. E-mail: nohad.gresh@parisdescartes.fr.

Notes

The authors declare no competing financial interest.

ACKNOWLEDGMENTS

We sincerely thank the Association Philippe Jabre for funding the Ph.D. research of Krystel El Hage. We thank the Grand Equipement National de Calcul Intensif (GENCI): Institut du Developement et des Ressources en Informatique Scientifique (IDRIS), Centre Informatique de l'Enseignement Supérieur (CINES), France, project No. x2009-075009), and the Centre de Ressources Informatiques de Haute Normandie (CRIHAN, Rouen, France), project 1998053. The authors also acknowledge the Research Council of Saint Joseph University of Beirut, Beirut, Lebanon (Project FS39), for financial support.

REFERENCES

(1) Lu, Y.; Shi, T.; Wang, Y.; Yang, H.; Yan, X.; Luo, X.; Jiang, H.; Zhu, W. Halogen Bonding - A Novel Interaction for Rational Drug Design? *J. Med. Chem.* **2009**, *52*, 2854−2862.

(2) Hernandes, M. Z.; Cavalcanti, S. M.; Moreira, D. R.; de Azevedo, W. F., Jr.; Leite, A. C. Halogen Atoms in the Modern Medicinal Chemistry: Hints for the Drug Design. *Curr. Drug Targets.* **2010**, *11*, 303−314.

(3) Matter, H.; Nazaré, M.; Güssregen, S.; Will, D. W.; Schreuder, H.; Bauer, A.; Urmann, M.; Ritter, K.; Wagner, M.; Wehner, V. Evidence for C-Cl/C-Br···π Interactions as an Important Contribution to Protein−Ligand Binding Affinity. *Angew. Chem., Int. Ed.* **2009**, *48*, 2911−2916.

(4) Clark, T.; Hennemann, M.; Murray, J. S.; Politzer, P. Halogen Bonding: the Sigma-Hole. *J. Mol. Mod.* **2007**, *13*, 291−296.

(5) Murray, J. S.; Lane, P.; Politzer, P. Expansion of the σ-Hole Concept. *J. Mol. Mod.* **2009**, *15*, 723−729.

(6) Politzer, P.; Murray, J. S.; Clark, T. Halogen Bonding: an Electrostatically-Driven Highly Directional Noncovalent Interaction. *Phys. Chem. Chem. Phys.* **2010**, *12*, 7748−7757.

(7) Hardegger, L. A.; Kuhn, B.; Spinnler, B.; Anselm, L.; Ecabert, R.; Stihle, M.; Gsell, B.; Thoma, R.; Diez, J.; Benz, J.; et al. Systematic Investigation of Halogen Bonding in Protein−Ligand Interactions. *Angew. Chem., Int. Ed.* **2011**, *50*, 314−318.

(8) Voth, A. R.; Ho, P. S. The Role of Halogen Bonding in Inhibitor Recognition and Binding by Protein Kinases. *Curr. Top. Med. Chem.* **2007**, *7*, 1336−1348.

(9) Voth, A. R.; Khuu, P.; Oishi, K.; Ho, P. S. Halogen Bonds as Orthogonal Molecular Interactions to Hydrogen Bonds. *Nat. Chem.* **2009**, *1*, 74−79.

(10) Auffinger, P.; Hay, F. A.; Westhof, E.; Ho, P. S. Halogen Bonds in Biological Molecules. *Proc. Natl. Acad. Sci. U. S. A.* **2004**, *101*, 16789−16794.
(11) Gresh, N.; Cisneros, A. G.; Darden, T. A.; Piquemal, J.-P. Anisotropic, Polarizable Molecular Mechanics Studies of Inter- and Intramolecular Interactions and Ligand−Macromolecule Complexes. A Bottom-Up Strategy. *J. Chem. Theory Comput.* **2007**, *3*, 1960−1986.
(12) Marchand, C.; Maddali, K.; Metifiot, M.; Pommier, Y. HIV-1 IN Inhibitors: 2010 Update and Perspectives. *Curr. Top Med. Chem.* **2009**, *9*, 1016−1037.
(13) Klibanov, O. M. Elvitegravir, an Oral HIV Integrase Inhibitor, for the Potential Treatment of HIV Infection. *Curr. Opin Invest. Drugs* **2009**, *10*, 190−200.
(14) Satom, M.; Motomura, T.; Aramaki, H.; Matsuda, T.; Yamashita, M.; Ito, Y.; Kawakami, H.; Matsuzaki, Y.; Watanabe, W.; Yamataka, K.; et al. Novel HIV-1 Integrase Inhibitors Derived from Quinolone Antibiotics. *J. Med. Chem.* **2006**, *49*, 1506−1508.
(15) Schafer, J. J.; Squires, K. E. Integrase Inhibitors: a Novel Class of Antiretroviral Agents. *Ann. Pharmacother.* **2010**, *44*, 145−156.
(16) Zolopa, A. R.; Berger, D. S.; Lampiris, H.; Zhong, L.; Chuck, S. L.; Enejosa, J. V.; Kearney, B. P.; Cheng, A. K. Activity of Elvitegravir, a Once-Daily Integrase Inhibitor, Against Resistant HIV Type 1: Results of a Phase 2, Randomized, Controlled Dose-Ranging Clinical Trial. *J. Infect. Dis.* **2010**, *201*, 814−822.
(17) Hare, S.; Gupta, S. S.; Valkov, E.; Engelman, A.; Cherepanov, P. Retroviral Intasome Assembly and Inhibition of DNA Strand Transfer. *Nature* **2010**, *464*, 232−236.
(18) Stevens, W. J.; Fink, W. Frozen Fragment Reduced Variational Space Analysis of Hydrogen Bonding Interactions. Application to the Water Dimer. *Chem. Phys. Lett.* **1987**, *139*, 15−22.
(19) Boys, S. F.; Bernardi, F. The Calculation of Small Molecular Interactions by the Differences of Separate Total Energies. Some Procedures with Reduced Errors. *Mol. Phys.* **1970**, *19*, 553−566.
(20) Simon, S.; Duran, M.; Dannenberg, J. J. How Does Basis Set Superposition Error Change the Potential Surfaces for Hydrogen-Bonded Dimers? *J. Chem. Phys.* **1996**, *105*, 11024−11031.
(21) Schmidt, M. W.; Baldridge, K. K.; Boatz, J. A.; Elbert, S. T.; Gordon, M. S.; Jensen, J. H.; Koseki, S.; Matsunaga, N.; Nguyen, K. A.; Su, S.; Windus, T. L.; Dupuis, M.; Montgomery, J. A. General Atomic and Molecular Electronic Structure System. *J. Comput. Chem.* **1993**, *14*, 1347−1363.
(22) Dunning, T. H. Gaussian Basis Sets for Use in Correlated Molecular Calculations. I. The Atoms Boron Through Neon and Hydrogen. *J. Chem. Phys.* **1989**, *90*, 1007−1023.
(23) Feller, D. The Role of Databases in Support of Computational Chemistry Calculations. *J. Comput. Chem.* **1996**, *17*, 1571−85.
(24) Riley, K. E.; Op't Holt, B. T.; Merz, K. M. Critical Assessment of the Performance of Density Functional Methods for Several Atomic and Molecular Properties. *J. Chem. Theory Comput.* **2007**, *3*, 407−433.
(25) Grimme, S. Semiempirical GGA-type Density Functional Constructed with a Long-Range Dispersion Correction. *J. Comput. Chem.* **2006**, *27*, 1787−99.
(26) Frisch, M. J.; Trucks, G. W.; Schlegel, H. B.; Scuseria, G. E.; Robb, M. A.; Cheeseman, J. R.; Scalmani, G.; Barone, V.; Mennucci, B.; Petersson, G. A.; Nakatsuji, H.; Caricato, M.; Li, X.; Hratchian, H. P.; Izmaylov, A. F.; Bloino, J.; Zheng, G.; Sonnenberg, J. L.; Hada, M.; Ehara, M.; Toyota, K.; Fukuda, R.; Hasegawa, J.; Ishida, M.; Nakajima, T.; Honda, Y.; Kitao, O.; Nakai, H.; Vreven, T.; Montgomery, J. A., Jr.; Peralta, J. E.; Ogliaro, F.; Bearpark, M.; Heyd, J. J.; Brothers, E.; Kudin, K. N.; Staroverov, V. N.; Kobayashi, R.; Normand, J.; Raghavachari, K.; Rendell, A.; Burant, J. C.; Iyengar, S. S.; Tomasi, J.; Cossi, M.; Rega, N.; Millam, N. J.; Klene, M.; Knox, J. E.; Cross, J. B.; Bakken, V.; Adamo, C.; Jaramillo, J.; Gomperts, R.; Stratmann, R. E.; Yazyev, O.; Austin, A. J.; Cammi, R.; Pomelli, C.; Ochterski, J. W.; Martin, R. L.; Morokuma, K.; Zakrzewski, V. G.; Voth, G. A.; Salvador, P.; Dannenberg, J. J.; Dapprich, S.; Daniels, A. D.; Farkas, Ö.; Foresman, J. B.; Ortiz, J. V.; Cioslowski, J.; Fox, D. J. *Gaussian 09*, Revision D.01; Gaussian, Inc.: Wallingford, CT, 2009.
(27) Stone, A. J. Distributed Multipole Analysis, or How to Describe a Molecular Charge Distribution. *Chem. Phys. Lett.* **1981**, *83*, 233−239.
(28) Stone, A. J.; Alderton, M. Distributed Multipole Analysis — Methods and Applications. *Mol. Phys.* **1985**, *56*, 1047−1064.
(29) Vigné-Maeder, F.; Claverie, P. The Exact Multicenter Multipolar Part of a Molecular Charge Distribution and its Simplified Representations. *J. Chem. Phys.* **1988**, *88*, 4934−4948.
(30) Piquemal, J.-P.; Gresh, N.; Giessner-Prettre, C. Improved Formulas for the Calculation of the Electrostatic Contribution to Intermolecular Interaction Energy from Multipolar Expansion of the Electronic Distribution. *J. Phys. Chem. A* **2003**, *107*, 10353−10359.
(31) Garmer, D. R.; Stevens, W. J. Transferability of Molecular Distributed Polarizabilities from a Simple Localized Orbital Based Method. *J. Phys. Chem.* **1989**, *93*, 8263−8270.
(32) Hage, K. E.; Piquemal, J.-P.; Hobaika, Z.; Maroun, R. G.; Gresh, N. Could an Anisotropic Molecular Mechanics/Dynamics Potential Account for Sigma Hole Effects in the Complexes of Halogenated Compounds? *J. Comput. Chem.* **2013**, *34*, 1125−1135.
(33) Creuzet, S.; Gresh, N.; Langlet, J. Adjustment of the SIBFA Method for Potential Maps to Study Hydrogen-Bondng Vibrational Frequencies. *J. Chim. Phys.* **1991**, *88*, 2399−2409.
(34) Kitaura, K.; Morokuma, K. A New Energy Decomposition Scheme for Molecular Interactions Within the Hartree-Fock Approximation. *Int. J. Quantum Chem.* **1976**, *10*, 325−340.
(35) Chai, J. D.; Head-Gordon, M. Long-Range Corrected Double-Hybrid Density Functionals. *J. Chem. Phys.* **2009**, *131*, 174105−174113.
(36) Zhao, Y.; Truhlar, D. G. The M06 Suite of Density Functionals for Main Group Thermochemistry, Thermochemical Kinetics, Noncovalent Interactions, Excited States, and Transition Elements: Two New Functionals and Systematic Testing of Four M06-Class Functionals and 12 Other Functionals. *Theor. Chem. Acc.* **2008**, *120*, 215−241.
(37) Bereau, T.; Kramer, C.; Meuwly, M. Leveraging Symmetries of Static Atomic Multipole Electrostatics in Molecular Dynamics Simulations. *J. Chem. Theory Comput.* **2013**, *9*, 5450−5459.
(38) Gresh, N. Model, Multiply Hydrogen-Bonded Water Oligomers (N = 3−20). How Closely Can a Separable, ab Initio-Grounded Molecular Mechanics Procedure Reproduce. *J. Phys. Chem. A* **1997**, *101*, 8680−94.
(39) Guo, H.; Gresh, N.; Roques, B. P.; Salahub, D. R. Many-Body Effects in Systems of Peptide Hydrogen-Bonded Networks and their Contributions to Ligand Binding: A Comparison of the Performances of DFT and Polarizable Molecular Mechanics. *J. Phys. Chem. B* **2000**, *104*, 9746−9754.
(40) Piquemal, J.-P.; Chelli, R.; Procacci, P.; Gresh, N. Key Role of the Polarization Anisotropy of Water in Modeling Classical Polarizable Force Fields. *J. Phys. Chem. A* **2007**, *111*, 8170−8176.
(41) Tiraboschi, G.; Gresh, N.; Giessner-Prettre, C.; Pedersen, L. G.; Deerfield, D. W. Parallel Ab Initio and Molecular Mechanics Investigation of Polycoordinated Zn(II) Complexes with Model Hard and Soft Ligands: Variations of Binding Energy and of Its Components With Number and Charges of Ligands. *J. Comput. Chem.* **2000**, *21*, 1011−1039.
(42) Tiraboschi, G.; Roques, B. P.; Gresh, N. Joint Quantum Chemical and Polarizable Molecular Mechanics Investigation of Formate Complexes with Penta- and Hexahydrated Zn^{2+}: Comparison Between Energetics of Model Bidentate, Monodentate, and Through-Water Zn^{2+} Binding Modes and Evaluation of Nonadditivity Effects. *J. Comput. Chem.* **1999**, *20*, 1379−1390.
(43) Chaudret, R.; Gresh, N.; Parisel, O.; Piquemal, J.-P. Many-Body Exchange-Repulsion in Polarizable Molecular Mechanics. I. Orbital Based Approximations and Application to Hydrated Metal Cations Complexes. *J. Comput. Chem.* **2011**, *31*, 2949−2957.
(44) Forni, A.; Pieraccini, S.; Rendine, S.; Sironi, M. Halogen Bonds with Benzene: an Assessment of DFT Functionals. *J. Comput. Chem.* **2014**, *3*, 386−394.
(45) Day, P. N.; Jensen, J. H.; Gordon, M. S.; Webb, S. P.; Stevens, W. J.; Krauss, M.; Garmer, D. R.; Cohen, D. An Effective Fragment

Method for Modelling Solvent Effects in Quantum Mechanical Calculations. *J. Chem. Phys.* **1996**, *105*, 1968−1986.
(46) Gordon, M. S.; Smith, Q. A.; Xu, P.; Slipchenko, L. V. Accurate First Principles Model Potentials for Intermolecular Interactions. *Annu. Rev. Phys. Chem.* **2013**, *64*, 553−578.